Atmospheric chemistry of $C_4F_9OC_2H_5$ (HFE-7200), $C_4F_9OCH_3$ (HFE-7100), $C_3F_7OCH_3$ (HFE-7000) and $C_3F_7CH_2OH$: Temperature dependence of the kinetics of their reactions with OH radicals, atmospheric lifetimes and Global Warming Potentials

Iván Bravo[1], Yolanda Díaz-de-Mera[1], Alfonso Aranda[1], Kevin Smith[2], Keith P. Shine[3] and George Marston[4]

[1] Physical Chemistry Department, University of Castilla–La Mancha Chemistry Faculty, Avda. Camilo Jose Cela 10, 13071 Ciudad Real, Spain

[2]Space Science and Technology Department, Rutherford Appleton Laboratory, Didcot, Oxon, OX11 0QX, UK

[3]Department of Meteorology, University of Reading, Earley Gate PO Box 243, Reading RG6 6BB, UK

[4]Department of Chemistry, University of Reading, Whiteknights, PO Box 224, Reading RG6 6AD, UK

Abstract

The atmospheric chemistry of several gases used in industrial applications, $C_4F_9OC_2H_5$ (HFE-7200), $C_4F_9OCH_3$ (HFE-7100), $C_3F_7OCH_3$ (HFE-7000) and $C_3F_7CH_2OH$ has been studied. The discharge flow technique coupled with mass-spectrometric detection has been used to study the kinetics of their reactions with OH radicals as a function of temperature. The infrared spectra of the compounds have also been measured. The following Arrhenius expressions for the reactions were determined (in units of cm^3 $molecule^{-1}$ s^{-1}): $k(OH + HFE\text{-}7200) = (6.9^{+2.3}_{-1.7}) \times 10^{-11} \exp(-(2030\pm190)/T)$; $k(OH + HFE\text{-}7100) = (2.8^{+3.2}_{-1.5}) \times 10^{-11} \exp(-(2200\pm490)/T)$; $k(OH + HFE\text{-}7000) = (2.0^{+1.2}_{-0.7}) \times 10^{-11} \exp(-(2130\pm290)/T)$; and $k(OH + C_3F_7CH_2OH) = (1.4^{+0.3}_{-0.2}) \times 10^{-11} \exp(-(1460\pm120)/T)$. From the infrared spectra, radiative forcing efficiencies were determined and compared with earlier estimates in the literature. These were combined with the kinetic data to estimate 100-year time horizon global warming potentials relative to CO_2 of 69, 337, 499 and 36 for HFE-7200, HFE-7100, HFE-7000 and $CF_3CF_2CF_2CH_2OH$, respectively.

1. Introduction

The adverse effect of chlorofluorocarbon (CFC) release into the atmosphere has been widely recognized and has led to the replacement of CFCs — often with hydroflurocarbons (HFCs) — in industrial processes. [1] Hydrofluoroethers (HFEs) and partially fluorinated alcohols have been suggested as substitutes for HFCs in a wide range of applications, such as refrigeration, carrier fluids for lubricants, and cleaning of electronic components.[2] and [3] Because these molecules do not contain Cl atoms, they do not contribute to ozone depletion but may contribute to global warming. It is important to improve our knowledge of the rate coefficients for their reactions with OH and the infrared spectroscopic properties of these compounds to accurately evaluate their environmental impact.

The primary removal process for HFEs and partially fluorinated organic compounds in the troposphere is reaction with OH radicals. An understanding of the kinetics of the reactions is therefore essential in the evaluation of the atmospheric lifetime of these molecules. Generally, atmospheric lifetime calculations are based on the OH radical reaction rate coefficients, assuming that reaction rates are independent of temperature.[4] However, for chemical species of low reactivity, a relatively homogeneous vertical distribution in the troposphere is expected. Thus, to a large extent, the losses of such chemicals take place at temperatures that are lower than 298 K. For reactions with relatively high activation energies, E_a, neglecting the temperature dependence of the kinetic rate coefficients may lead to underestimates of the corresponding lifetimes. Thus, knowledge of the temperature dependence for the rate coefficients of these reactions becomes necessary.

Since halocarbons, HFEs and fluorinated alcohols absorb infrared (IR) radiation, it is also necessary to determine their IR absorption spectra if their climate impact is to be assessed. Combining the IR spectra with information about the transmission behaviour of the atmosphere allows radiative forcings — and the radiative efficiencies per unit concentration — to be determined. When, in turn, these radiative efficiencies are combined with atmospheric lifetimes, Global Warming Potentials (GWPs) can be estimated for any chosen timescale, as described, for example, by Pinnock et al. 1995.[5]

In order to improve our knowledge of the atmospheric chemistry of HFEs and fluorinated alcohols in general — and HFE-7200, HFE-7100, HFE-7000 and its structural isomer $C_3F_7CH_2OH$ in particular — we have carried out a kinetic study of the following reactions, using an absolute technique at 1 Torr of total pressure:

$C_4F_9OCH_2CH_3$ (HFE-7200[a]) + OH → Products (1)

$C_4F_9OCH_3$ (HFE-7100[b]) + OH → Products (2)

$CF_3CF_2CF_2OCH_3$ (HFE-7000[c]) + OH → Products (3)

$CF_3CF_2CF_2CH_2OH$ + OH → Products (4)

For these reactions, we report rate coefficients and their temperature dependence in the range 288-368 K, allowing us to determine atmospheric lifetimes for the four compounds. We have also measured the IR spectra of the three HFEs and the alcohol, and are able to estimate radiative forcing efficiencies and global warming potentials from our results. We also compare our measurements and calculations with previous work.

This work is the first to report direct measurements at low pressures of the temperature dependence of the kinetics of the reactions of OH with HFE-7200, HFE-7000 and $C_3F_7CH_2OH$; a single study has examined the temperature dependence of the kinetics of the reaction of OH with HFE-7000 using direct methods at moderate pressures.[6] A few previous studies have reported the radiative forcing efficiencies and GWPs of the molecules investigated here, but experience has indicated that quite divergent values can be found in the literature for the same gases (see e.g. Forster et al. 2005[7]); also, as will be shown, the tabulations of the GWPs for these molecules in the Intergovernmental Panel on Climate Change (IPCC)[8] and related scientific assessments are often based on very simplified estimates which are in need of updating.

2. Experimental section

2.1. Kinetics

Kinetic experiments were carried out in a discharge flow-mass spectrometry system (DF-MS) which is shown schematically in Figure 1. The design and performance of the sampling and detection system have been described previously.[9] and [10] The system was improved recently introducing the additional high-vacuum chamber between the reactor and the high-vacuum chamber containing the quadrupole mass spectrometer (Pfeiffer Prisma).[11] The pressures in the two chambers are typically 1×10^{-6} Torr and 1×10^{-8} Torr, respectively. The molecular species are sampled from the reactor to the first vacuum chamber through a stainless steel cone with a

[a] HFE-7200 is sometimes referred to as HFE-569sf2 and is a mixture of $(CF_3)_2CFCF_2OCH_2CH_3$ and $CF_3CF_2CF_2CF_2OCH_2CH_3$

[b] HFE-7100 is sometimes referred to as HFE-449s1 and is a mixture of $(CF_3)_2CFCF_2OCH_3$ and $CF_3CF_2CF_2CF_2OCH_3$

[c] HFE-7000 is sometimes referred to as HFE-347mcc3

250 μm diameter orifice and enter the vacuum chamber containing the detection system through a second steel cone with an orifice of 1000 μm diameter.

OH production

The OH radicals were produced in region (1) in Figure 1 by reaction of F atoms with H_2O in excess:

$F + H_2O \rightarrow OH + HF$ (5)

$k_5 = 1.4 \times 10^{-11} \exp[(0 \pm 200)/T]$ cm^3 molecule^{-1} s^{-1} (240 - 373K)[12]

Atomic fluorine was generated in a microwave discharge of F_2/He mixtures joined to the main reactor through inlet 1. The discharge tube contained an alumina sleeve to enhance F_2 dissociation (dissociation yield, generally within 45-65%) and to reduce the F-atom wall losses. The inner surfaces of the reactor and the movable injector were coated with halocarbon wax. The absolute concentration of F atoms and its losses were determined by titration with Br_2, measuring the decrease in the Br_2 signal:

$F + Br_2 \rightarrow BrF + Br$ (6)

$k_6 = 2.16 \times 10^{-10}$ cm^3 molecule^{-1} s^{-1} [13]

To determine the losses of F atoms in region (1), Br_2 was introduced through inlet 1a and inlet 2, successively, thus allowing the determination of the F-atom concentration at the beginning and at the end of this region. The rate constant for wall losses of F atoms in region (1) was determined as 50 ± 10 s^{-1} (mean value). Typical concentrations for F atoms at the beginning of region (1) were $[F]_0 = (2 - 6.5) \times 10^{12}$ molecule cm^{-3}.

A large excess of H_2O (inlet 1a) was used to ensure the formation of OH. With $[H_2O] \approx (50 - 100) \times [F]_0$ and at flow velocities inside the injector of around 2400 cm s^{-1}, the formation of OH is completed in approximately 5 cm at room temperature in region (1) (region 1 is 13.5 cm long).

The major complications in the generation of OH are the following reactions, which could lead to the undesirable presence of O atoms in the reactor:

$OH + OH \rightarrow H_2O + O$ (7)

$k_7 = 6.2 \times 10^{-14} (T/298)^{2.6} \exp(945/T)$ cm^3 molecule^{-1} s^{-1} (200 - 350K)[12]

$O + OH \rightarrow O_2 + H$ (8)

$k_8 = 2.4 \times 10^{-11} \exp(110/T)$ cm^3 molecule^{-1} s^{-1} (150 - 500K)[12]

The contribution of these two reactions to O-atom formation in region (1) was evaluated together with the OH source reaction (5) and the wall losses of F and OH in a numerical kinetic

model (FACSIMILE program) using the same conditions as in the experiments. At the end of region (1), the concentration of O atoms was found to be much lower than that of OH radicals (*ca*. 30 times). Once in the main reactor (region 2), bimolecular reactions between radicals, (7) and (8), are even less important due to the dilution of the species coming from the injector with the carrier gas (inlet 2). Furthermore, reactions with O atoms are generally much slower than OH reactions for ethers and alcohols.[12], [14], [15], [16]and [17] Consequently, under our experimental conditions, the effect of O-atom formation on the kinetic measurements can be considered negligible.

The quantification of OH radicals in region (2), considering the dilution effect in this region from region (1), was achieved using the reaction of OH with an excess of Br_2, where $[OH]_0=\Delta[Br_2]$,

$OH + Br_2 \rightarrow HOBr + Br$ (9)

$k_9 = 1.9 \times 10^{-11} \exp(240/T)$ cm^3 molecule^{-1} s^{-1} (230-360K)[12]

Br_2 was added in excess upstream of region (2) at inlet 2, and the depletion of the Br_2 was measured by monitoring its peak at *m*/*e* = 160. With our experimental arrangement, typical $[OH]_0$ was (1 - 2) × 10^{12} molecule cm^{-3}.

OH reactions in the flow tube

The reaction between OH radicals and the organic compounds added at inlet 2 takes place in region (2) for different total reaction times. The reaction time resolution was achieved by changing the position of the sliding injector. For a given position of the injector (reaction time) the extent of the reaction was measured by scavenging the remaining OH radicals by the fast reaction with I_2, which was held in large excess:

$I_2 + OH \rightarrow HOI + I$ (10)

$k_{10} = 2.1 \times 10^{-10}$ cm^3 molecule^{-1} s^{-1} (240-350K)[12]

The HOI molecules generated in this way were followed at their peak at *m*/*e* = 144 during the kinetic run with an OH radical detection limit of 5 × 10^{10} molecule cm^{-3}. Molecular iodine was fed into the reactor via inlet 3 by flowing helium through a column containing I_2 crystals. (Reaction (9) was not used to follow OH since we found contributions from the fluorinated compounds in the peaks at *m/e* = 96 and 98, which are the HOBr molecular peaks).

The experimental conditions for the kinetic studies are summarized in Table 1. All experiments were carried out at 1 Torr total pressure within the temperature range of 288-368 K and under pseudo-first-order conditions, with the organic compound in excess over OH radicals.

Preliminary experiments were conducted in which the reactions between F_2, I_2 and H_2O with the organic compounds were evaluated: no reaction was observed within the time scale used in the experiments.

The flows of the helium carrier gas in regions (1) and (2) were regulated and measured with calibrated mass-flow controllers. Some of the reactants (Br_2, F_2, H_2O) were diluted in helium and stored in bulbs of known volumes. Their flow rates were obtained from the decrease of the pressure bulbs with time. In the case of the fluorinated organic compounds, they were used without dilution to reach higher concentrations. To ensure constant and accurate concentrations of the fluorinated organic compounds, their flows were also regulated with mass-flow controllers. The HFEs and $C_3F_7CH_2OH$ were introduced into the reactor through inlet 2 but the detection of their parent peaks was not possible since the mass spectrometer only detects masses up to 200 amu. However the signals found at *m/z* = 131, 69, 119 and 131 for HFE-7200, HFE-7100, HFE-7000, and $C_3F_7CH_2OH$, respectively, showed good intensities and no overlap with the peaks of the rest of the species in the reactor.

For a bimolecular reaction between OH radical and an organic compound under pseudo-first-order conditions, the integrated equation that applies is as follows:

$$ln[OH]_t = ln[OH]_0 - k't \qquad \text{(I)}$$

where k' is the pseudo-first-order kinetic rate constant, $k' = k + k_w$, with k_w being the heterogeneous wall loss rate constant in the reactor and k the bimolecular kinetic rate constant. The heterogeneous wall losses of OH radicals in the reactor were evaluated in separate experiments carried out in the absence of organic compound by monitoring the formation of HOI. In these experiments, HOI was measured for different positions of the injector (thus changing the contact time of OH with the reactor wall) with I_2 coming from inlet 3. A similar value was obtained for all temperatures studied (288-368 K) with an average value of $k_w = 20 \pm 8$ s^{-1}.

2.2. Infrared spectra

Infrared spectra were measured at the Molecular Spectroscopy Facility (MSF) at the Rutherford Appleton Laboratory (RAL).[18] Measurements were obtained at 298 K using a Bruker IFS 125 HR spectrometer in the range 600-1800 cm^{-1} with a 5 cm stainless steel cell fitted with KBr windows. The spectrometer was operated at a spectral resolution of 0.03 cm^{-1} (for HFE-7000) or 0.1 cm^{-1} (other compounds) with interferograms being obtained from 50 co-added scans. Spectra were recorded either of the pure vapor or in the presence of 60 – 506 hPa of N_2 diluent. Wide and narrow band MCT detectors, with long wave cut-offs of 500 and 800 cm^{-1}, were used

to measure spectra in the 700 – 1400 cm^{-1} region using a KBr beam splitter and globar infrared source.

In all experiments, pure compounds were transferred to a small glass vial via a welded stainless steel gas line and degassed by freeze/pump/thaw cycles before use. For the measurements of the pure vapour, the desired quantity of material was allowed into the cell, and the pressure monitored throughout the recording of the spectrum.

The mixtures in nitrogen were made up in 1000 cm^3 capacity glass bulbs. The compounds of interest was allowed into the bulb to a pressure of about 0.33-1.33 hPa and then made-up with nitrogen (~1000 hPa). Bulbs of the compound of interest in N_2 were mixed in this way and allowed to stand overnight to allow good mixing of the two gases.

To ensure that saturation was not a problem in the measurements, for each compound, the peak absorbance was plotted as a function of pressure. Points at higher pressures showing non-linear behaviour were ignored and absorption cross sections were derived from the slopes of the linear portions of the plots. The spectra were then normalized to this value for the cross section and the integrated absorption cross section calculated from the average of the spectra. The absorption cross section, at temperature, *T*, wavenumber $\bar{\nu}$ (cm^{-1}) and at the experimental resolution was determined through the relationship:

$$\sigma(\bar{\nu},T) = \ln(I_0 / I) / cl$$

where $\sigma(\bar{\nu},T)$ is the absorption cross section in cm^2 $molecule^{-1}$ at temperature, *T*, and wavenumber, $\bar{\nu}$; I_0 is the intensity of radiation reaching the detector when the cell is empty; *I* is the intensity of radiation reaching the detector when the cell contains sample; *c* is the concentration of sample (molecule cm^{-3}); and *l* is the pathlength (cm). Integrated absorption cross sections, *S*(*T*) in cm^2 $molecule^{-1}$ cm^{-1} were determined according to the expression:

$$S(T) = \int_{\bar{\nu}_1}^{\bar{\nu}_2} \sigma(\bar{\nu},T)\,\mathrm{d}\bar{\nu}$$

2.3 Reagents

The purities of the gases used were as follows: He (Praxair, 99.999%), F_2 (Praxair, 5% in Helium), Br_2 (Fluka, 99,5%), I_2 (Fluka, ≥99.5%), H_2O (Direct-Q, Millipore), HFE-7200 (3M Novec, >99%, consisting of 39% of isomer $CF_3CF_2CF_2CF_2OC_2H_5$ and 61% of isomer $(CF_3)_2CFCF_2OC_2H_5$), HFE-7100 (3M, ≥99%, consisting of 37% of isomer $CF_3CF_2CF_2CF_2OCH_3$

and 63% of isomer $(CF_3)_2CFCF_2OCH_3$), and HFE-7000 (3M Novec, >99%, consisting of 100% of isomer $CF_3CF_2CF_2OCH_3$), and 2,2,3,3,4,4,4 heptafluoro-1butanol (Aldrich, 99.1%).

3. Results and Discussion

3.1 Kinetics

In Figure 2, typical pseudo-first-order decays of OH versus time for reaction (4) are shown. Similar plots are obtained for the other compounds studied in this work. The experimental values of *k*' obtained from the slopes were corrected to take into account the axial and radial diffusion of OH atoms.[19] The effective diffusion coefficients of OH in He were calculated from the volumes of atomic diffusion.[20] The values obtained within the temperature range used (288-368 K) were $D_{OH/He}$ = 740-1550 $cm^2\ s^{-1}$ introducing corrections on *k*' of < 24 %, <10%, <9%, and <16%, for reactions (1), (2), (3), and (4), respectively.

The second-order rate constants for the studied reactions were calculated by plotting the corrected pseudo-first-order constants *vs.* the concentration of the molecule and applying weighted linear least-squares fittings as shown in Figure 3. At room temperature, the measured rate constants are $k_1 = (7.32\pm0.55) \times 10^{-14}$ cm^3 $molecule^{-1}$ s^{-1}, $k_2 = (1.49\pm0.13) \times 10^{-14}$ cm^3 $molecule^{-1}$ s^{-1}, $k_3 = (1.54\pm0.05) \times 10^{-14}$ cm^3 $molecule^{-1}$ $s^{-1,}$ and $k_4 = (1.07\pm0.05) \times 10^{-13}$ cm^3 $molecule^{-1}$ s^{-1}, with quoted errors at 2σ. In table 2 we summarize the results for all experimental conditions.

For all reactions, the reaction rate constants were found to increase with increasing temperature, as shown in Figure 4 in the form of Arrhenius plots. The linear weighted least-squares analysis of the data yield the activation energies and the pre-exponential factors, and allow the calculation of the kinetic rate constants through the following equations in the specified range of temperature at 1 Torr total pressure (quoted uncertainties represent 2σ):

$k_1 = (6.9^{+2.3}_{-1.7}) \times 10^{-11} \exp(-(2030\pm190)/T)$ cm^3 $molecule^{-1}$ s^{-1} T = 288-368 K

$k_2 = (2.8^{+3.2}_{-1.5}) \times 10^{-11} \exp(-(2200\pm490)/T)$ cm^3 $molecule^{-1}$ s^{-1} T = 288-368 K

$k_3 = (2.0^{+1.2}_{-0.7}) \times 10^{-11} \exp(-(2130\pm290)/T)$ cm^3 $molecule^{-1}$ s^{-1} T = 288-368 K

$k_4 = (1.4^{+0.3}_{-0.2}) \times 10^{-11} \exp(-(1460\pm120)/T)$ cm^3 $molecule^{-1}$ s^{-1} T = 290-368 K

It was not possible to study reactions (1) to (4) at lower temperatures due to the significant increase in the heterogeneous losses of OH radical.

A number of studies examining the kinetics of the title reactions have been carried out previously and are summarized in Table 3. Our result at 298 K for $C_4F_9OC_2H_5$ (HFE-7200) + OH (1) is in excellent agreement (within a few per cent of the weighted average for the two isomers) with that obtained by Christensen *et al.*[21] and a little lower (<30 %) than the value obtained by Oyaro and Nielsen[22]. When systematic errors are taken into consideration, this difference may not be significant; such errors are particularly associated with relative rate measurements because of the uncertainty in the value of the rate coefficient for the reference compound. For reaction (2), $C_4F_9OCH_3$ (HFE-7100) + OH, the measured kinetic rate constant is some 25 % higher than the approximate value reported by Wallington *et al.*[23] and within one per cent of the value reported by Oyaro and Nielsen.[22] The value reported by Cavalli *et al.*[24] is significantly lower (40 – 50 %) than the other measurements. For reaction (3), $C_3F_7OCH_3$ (HFE-7000) + OH, reported values from previous studies for the *n*-isomer[6] and [25] are somewhat lower (<25 %) than our value, although the single reported value for the *i*-isomer is in very good agreement with our measurement.[6] Finally, the value reported in this work for reaction (4), $C_3F_7CH_2OH$ + OH, is in excellent agreement — better than a few per cent difference — with the single previous study of Hurley *et al.*[26].

Our experiments were carried out under very different conditions from those of the previous studies of the kinetics of the title reactions. In particular, the total pressure was significantly lower than the pressures used in previous studies. With the exception of the anomalously low rate coefficient reported by Cavalli *et al.*[24] for the reaction of OH with HFE-7100, all reported values are in agreement within the expected error limits for kinetic measurements. We conclude, therefore, that the kinetics of these reactions are independent of pressure, as expected for a direct abstraction reaction.

This study is the first to investigate the temperature dependence of the kinetics of the reactions of OH with HFE-7200, HFE-7100 and $C_3F_7CH_2OH$. There is a single previous study of the temperature dependence of the kinetics of the reaction of OH with HFE-7000, carried out by Tokuhashi *et al.*[6]. In general, the rate constants determined here for the reaction of OH with HFE-7000 are larger by about 20 – 30 % than those determined by Tokuhashi *et al.*, with the discrepancy being largest at lower temperatures; we have determined a larger activation barrier (17.3 kJ mol^{-1} *vs.* 12.7 kJ mol^{-1}) and pre-exponential *A* factor (2.0×10^{-11} cm^3 molecule^{-1}s^{-1} *vs.* 2.1×10^{-12} cm^3 molecule^{-1}s^{-1}) than those determined by Tokuhashi *et al.* [6] It is not clear what the source of this discrepancy is. There have also been studies of the temperature dependences of the kinetics of the reactions of OH with other HFEs fluorinated alcohols.[6], [27], [28] and [29]. In these studies, the rate constants showed a significant dependence on temperature.

$C_4F_9OCH_3$ and $C_3F_7OCH_3$ are part of a series of compounds that can be written as $C_nF_{2n+1}OCH_3$. In Table 3 we present the data in the literature for these reactions with n = 3 and 4. Other

authors have studied the $C_nF_{2n+1}OCH_3$ + OH reactions with lower values for *n*. Tokuhashi *et al.*[6] reported $k = (1.21\pm0.09) \times 10^{-14}$ cm^3 $molecule^{-1}$ s^{-1} for *n*=2. For n=1, Zhang *et al.*[30] reported $k = (2.14\pm0.15) \times 10^{-14}$ cm^3 $molecule^{-1}$ s^{-1}, Orkin *et al.*[31] reported $k = (1.3\pm0.09) \times 10^{-14}$ cm^3 $molecule^{-1}$ s^{-1}, Hsu *et al.*[29] reported 1.0×10^{-14} cm^3 $molecule^{-1}$ s^{-1}, and Chen *et al.*[28] reported $k = (1.19\pm0.14) \times 10^{-14}$ cm^3 $molecule^{-1}$ s^{-1}. In broad terms, we can conclude that for reactions of $C_nF_{2n+1}OCH_3$ (for *n* = 1-4) with OH, the kinetic rate constants are independent of the number of $-CF_2-$ in the perfluorinated chain. Similar behaviour has been observed for the reactions of Cl with $C_nF_{2n+1}OCH_3$ compounds.[32]

As with the $C_nF_{2n+1}OCH_3$ series, several authors have studied $C_nF_{2n+1}CH_2OH$ + OH reactions with different values for *n*. Hurley *et al.* [26] reported no dependence of the rate constant on *n* for *n* = 1 – 4, reporting an average value of $k = (1.02 \pm 0.10) \times 10^{-13}$ cm^3 $molecule^{-1}$ s^{-1}. For *n* = 1, the following results have been reported: $k = (9.55 \pm 0.71) \times 10^{-14}$, $(1.00 \pm 0.04) \times 10^{-13}$, and $(1.06 \pm 0.30) \times 10^{-13}$ cm^3 $molecule^{-1}$ s^{-1} by Wallington *et al.* [33], Tokuhashi *et al.* [27] and Kovacs *et al.*[34], respectively. For *n*=2, the following results have been reported: $k = (1.02 \pm 0.04) \times 10^{-13}$, and 1.11×10^{-13} cm^3 $molecule^{-1}$ s^{-1} by Tokuhashi *et al.*[6] and Chen *et al.*[35] , respectively. Our value for *n* = 3 is consistent with these data. Taken together, the results show that for fluorinated alcohols, the kinetic rate constant for the reaction with OH is independent of the number of $-CF_2-$ moieties in the perfluorinated chain.

For the hydrogenated part of the title fluorinated ether compounds, the replacement of a methyl group by an ethyl group leads to a substantial increase in reactivity towards OH radicals, with k_1 around 5 times larger than k_2 and k_3 (at 298 K, Table 2). These observations have interesting implications for the design of chemical structures with particular industrial applications in mind. The length (and branching) of the fluorinated part of the ether may be substantially modified to provide the desired physico-chemical behaviour. On the other hand, the alkyl part may be modified to increase the gas-phase reactivity and hence ensure efficient elimination from the troposphere.

Furthermore, the reactivity may be significantly modified by changing the nature of the functional group in the molecule as shown by the results obtained for the isomeric compounds HFE-7000 and $C_3F_7CH_2OH$, with the room temperature rate constant for the alcohol being an order of magnitude larger than for the ether (at 298 K, Table 2). Similar behaviour has been reported for the reactions of other fluorinated ethers and their isomeric fluorinated alcohols with OH radicals; for example $CF_3CH_2OCH_3$ / $CF_3CH_2CH_2OH$ and CHF_2OCH_3 / CHF_2CH_2OH have rate constant values of $(5.7\pm0.8) \times 10^{-13}$ / $(1.09\pm0.05) \times 10^{-12}$ and 5.96×10^{-14} / $(4.51\pm0.06) \times 10^{-13}$ cm^3 $molecule^{-1}$ s^{-1}, respectively. [36], [37], [38] and [39]

For alcohol molecules, H atoms in the -CH_2- and –OH groups are both reactive sites. Generally, OH radicals will tend to abstract the most weakly bound hydrogen atom in the molecule. For example, it has been shown that the CH_3CH_2OH + OH reaction occurs mainly (75-90%) *via* H-atom abstraction from the -CH_2- group,[12] as a consequence of the activating influence of the -OH group. This activating effect may also occur for $C_3F_7CH_2OH$ explaining the higher value of k_4 compared to k_3.

3.2 Atmospheric Lifetimes

Rate coefficients for the reactions of a given organic compound with the different oxidants in the atmosphere can be combined with measured, computed or estimated tropospheric concentrations of these species to provide lifetimes with respect to any of these potential transformation processes. Such calculated lifetimes depend on the assumed temperature (or, equivalently, the altitude) and on the concentrations used. From the data reported in this work for the rate constants and the Arrhenius parameters for reactions (1) to (4) listed in Table 2, gas-phase lifetimes can be obtained for HFE-7200, HFE-7100, HFE-7000 and $C_3F_7CH_2OH$. An alternative approach has been presented by Kurylo and Orkin[4] who estimated lifetimes with respect to gas-phase removal by OH, using methyl chloroform as reference:

$$\tau_{OH} = \frac{k_{OH}^{CH_3CCl_3}(272\,K)}{k_{OH}(272\,K)}\tau_{OH}^{CH_3CCl_3} \qquad \text{(II)}$$

where τ_{OH} and $\tau_{OH}^{CH_3CCl_3}$ (=5.99 year)[4] are the lifetimes of a given compound and CH_3CCl_3, respectively, due to the reactions with hydroxyl radical in the troposphere; k_{OH}(272 K) and $k_{OH}^{CH_3CCl_3}$ (272 K) (= 6.0×10^{-15}cm^3 molecule^{-1} s^{-1})[4] are the rate constants for the reactions of these compounds with OH at 272 K.[4] Rate coefficients at 272 K rather than at 298 K are used to reflect the fact that the average temperature of the troposphere is somewhat lower than room temperature. The atmospheric loss of the compounds of interest here is determined by reaction with OH radicals, and so the lifetime with respect to reaction with OH can be equated to the atmospheric lifetime.

As explained earlier, rate coefficients could not be determined at 272 K. However, it has been found that, for H-abstraction reactions of saturated compounds such as alkanes or fluorinated alkanes with OH, the Arrhenius equations in its linearized form (*ln k* vs. (1/*T*)) properly fits the experimental data in the temperature range 240-370K.[40], [41], [31] and [42] We are able therefore to confidently extrapolate our results to 272 K, and thus obtain atmospheric lifetimes at temperatures typical of the troposphere. Because of the lack of kinetic data for the temperature dependence of the kinetics of the reactions of OH with organic compounds, literature estimates

of atmospheric lifetimes often use rate constants obtained at 298 K, using $\tau = 1/k[OH]$, with [OH] = 1×10^6 molecule cm^{-3} as the average tropospheric concentration.[43] In Table 4 we show the atmospheric lifetimes with respect to reaction with OH or each of the compounds at 298 K and 272 K. It is clear that the use of rate coefficients determined at 298 K leads to underestimates of the lifetimes by up to a factor of two, which have knock-on effects on the determination of GWPs. For HFE-7000, our preferred lifetime is based on the average value for k_3(272 K) from this work and that of Tokuhashi *et al.*,[6] which gives 4.8 yr and is used in our calculation of GWPs.

3.3 Infrared Absorption Cross-section Measurements

Infrared spectra for HFE-7000, HFE-7100, HFE-7200, and $C_3F_7CH_2OH$ are illustrated in Figure 5. As expected, all spectra show strong bands at the C-F stretching region between 1200 – 1300 cm^{-1}, with maximum absorption cross sections in the region of $2 - 4 \times 10^{-18}$ cm^2 $molecule^{-1}$. Plots of absorbance *vs.* pressure are illustrated in Figure 6; they show good linearity and zero intercepts (within error). Integrating the spectra between 700 and 1400 cm^{-1} gives the integrated absorption cross sections listed in Table 5. Error limits are based on the root mean square of the statistical errors (95 % confidence) from the absorbance *vs.* pressure plots and an estimated 15 % systematic error. (Statistical errors were determined as 21 %, 19 %, 4 % and 10 % for HFE-7000, HFE-7100, HFE-7200 and $C_3F_7CH_2OH$, respectively.) The accuracy of the reported absorption cross-sections are determined by uncertainties in concentrations, temperatures, optical pathlength and the photometric accuracy of the FTIR spectrometer.[44]

The values here are compared with others in the literature, although this is not straightforward, as different combinations of isomers are sometimes used. For HFE-7200, to our knowledge only one cross-section for this molecule is presented in the literature; Christensen *et al.*[21] show spectra for this gas, but do not report its integrated cross-section, although Sihra *et al.*[45] report a value of 36.56×10^{-17} cm^2 $molecule^{-1}$ cm^{-1} for the measurement by the same group. This value agrees, within the uncertainty bars of 10-20%, with our value of 38.6×10^{-17} cm^2 $molecule^{-1}$ cm^{-1}.

For HFE-7100, Wallington *et al.*[23] show spectra for this molecule. The integrated cross-section given by Sihra *et al.*[45] using measurements by the same group is 36.04×10^{-17} cm^2 $molecule^{-1}$ cm^{-1}; they also show that the integrated cross-sections of the two isomers of this molecule vary by about 10%. Cavalli *et al.*[24] report a considerably higher value of 42.3×10^{-17} cm^2 $molecule^{-1}$ cm^{-1}. Our value of 34.5×10^{-17} cm^2 $molecule^{-1}$ cm^{-1} is thus much closer to the Sihra *et al.*[45] value.

For HFE-7000, two prior measurements are known to us. Imasu *et al.*[46] (who refer to this molecule as mp04) report a value of 29.5×10^{-17} cm^2 molecule^{-1} cm^{-1}. Ninomiya *et al.*[25] show spectra for this molecule, and the integrated cross-section, using measurements by the same group, is given by Young *et al.*[47] as 28.6×10^{-17} cm^2 molecule^{-1} cm^{-1}. Our value of 28.1×10^{-17} cm^2 molecule^{-1} cm^{-1} thus agrees well these earlier values.

For $CF_3CF_2CF_2CH_2OH$, Sellevåg *et al.*[48] report a value of 21.9×10^{-17} cm^2 molecule^{-1} cm^{-1} in excellent agreement with our value of 21.5×10^{-17} cm^2 molecule^{-1} cm^{-1}.

3.4 Radiative Forcing Efficiencies

In the context of estimating the climate impact of the emissions of these gases, a fundamental parameter is the radiative forcing per unit concentration change, or radiative forcing efficiency (RE); this measures the change in the Earth's radiation balance for a 1 ppbv increase in concentration of the gas. For any gas, this efficiency depends on the spectral variation of the absorption cross-section, as the energy available to be absorbed in the atmosphere depends on this *via* both the Planck function and the absorption spectra of other species in the atmosphere (see, for example, Pinnock *et al.*[5]).

Here we adopt the simple method proposed by Pinnock *et al.*[5] where the absorption cross-section is integrated over 10 cm^{-1} intervals and multiplied by the RE in the same interval – the sum of all the efficiencies over all wavenumbers is likely to be accurate to about 10% for a gas that is well mixed throughout the atmosphere. We report such well-mixed values; however, the relatively short-lived species discussed here are unlikely to be well-mixed, and in particular their mixing ratios will fall off rapidly in the stratosphere. The actual distribution would likely depend on the location of the emissions which would require sophisticated chemical-transport model calculations to ascertain. Here we adopt the lifetime-correction suggested by Sihra *et al.*,[45] which was based on fits to such chemical-transport model calculations, whereby the well-mixed RE is multiplied by a factor $(1\text{-}0.24\tau^{-0.358})$, where τ is the atmospheric lifetime (see Section 3.2), to generate our final recommended value. Since the values of the RE presented within IPCC Assessment Reports (e.g. Forster et al.[8]) are used in the calculation of the GWP (see Section 3.5), we pay particular attention to how our values compare with the IPCC values.

For HFE-7200, the Forster *et al.*[8] value of 0.3 W m^{-2} ppbv^{-1} originates from the value presented in the 1998 WMO report[49]; this took the Christensen *et al.*[21] estimate (which had used the simple Pinnock *et al.* method[5]) of 0.39 W m^{-2} ppbv^{-1} and multiplied this by 0.8 to crudely account for the lifetime-dependence of the RE to report a value of 0.30 W m^{-2} ppbv^{-1} (although it should have been 0.31 W m^{-2} ppbv^{-1}). Sihra *et al.*[45] reported a value of 0.41 W m^{-2} ppbv^{-1} for a constant profile and 0.303 W m^{-2} ppbv^{-1} applying their lifetime correction. Our constant-

profile value of 0.42 W m^{-2} $ppbv^{-1}$ and 0.31 W m^{-2} $ppbv^{-1}$ using the lifetime correction are thus in good agreement with the Forster *et al.*[8] value.

For HFE-7100, the Forster *et al.*[8] value of 0.31 W m^{-2} $ppbv^{-1}$ originated from the WMO[49] value whereby the Wallington *et al.*[23] value of 0.37 W m^{-2} $ppbv^{-1}$ is multiplied by 0.8 to yield a reported lifetime-corrected value of 0.31 W m^{-2} $ppbv^{-1}$ (although it should have been 0.30 W m^{-2} $ppbv^{-1}$). Sihra *et al.*[45] reported a constant-profile value of 0.402 W m^{-2} $ppbv^{-1}$ and a lifetime corrected value of 0.347 W m^{-2} $ppbv^{-1}$. Our constant profile value is 0.36 W m^{-2} $ppbv^{-1}$ is slightly lower than that of Wallington *et al.*[23], consistent with our lower integrated absorption cross-section (see Section 4.2) and is 0.31 W m^{-2} $ppbv^{-1}$ when the lifetime correction is applied. This value is in good agreement with the value used in Forster *et al.*[8] although the Sihra *et al.*[45] value suggests that a value around 10% higher could also be adopted.

For HFE-7000, Forster *et al.*[8] use a value of 0.34 W m^{-2} $ppbv^{-1}$. The origin of this value is quite complex. Imasu *et al.*[46] derived an RE value for a clear-sky mid-latitude profile, which is not appropriate for the global-mean including clouds. WMO (1998)[49] took the ratio of the HFE-7000 to CFC-11 RE from Imasu *et al.*[46] and then multiplied this by their estimate of the CFC-11 RE to obtain the cloudy-sky global mean. No lifetime correction was employed. The constant-profile value derived here is 0.37 W m^{-2} $ppbv^{-1}$ and 0.32 W m^{-2} $ppbv^{-1}$ when lifetime-corrected; while this is close to the Forster *et al.*[8] value, the derivation here uses a more robust methodology. Young *et al.*[47] report a constant-profile value of 0.348 W m^{-2} $ppbv^{-1}$ using the simple Pinnock *et al.*[5] method. This is in reasonable agreement with the value derived here, but given that their integrated absorption cross-section is slightly higher (see Section 4.2), it is unclear why their RE is lower; this might reflect differences in the spectral variation of the absorption cross-section.

$CF_3CF_2CF_2CH_2OH$ is not reported in Forster *et al.*.[8] The only previous value known to us is from Sellevåg *et al.*[48] who use the simple Pinnock *et al.*[5] method, finding a constant-profile value of 0.295 W m^{-2} $ppbv^{-1}$. This compares well with our value of 0.28 W m^{-2} $ppbv^{-1}$, as expected from the similarity in integrated absorption cross-sections (Section 4.2). Our lifetime corrected value is 0.20 W m^{-2} $ppbv^{-1}$.

3.5 Global Warming Potentials

The GWP is one method for calculating the carbon-dioxide equivalent of a 1 kg emission of a gas – it takes into account both the lifetime and the RE of a gas. It is the radiative forcing of an emission of 1 kg at time zero, integrated over some given time horizon, divided by the same value for a 1 kg emission of carbon dioxide. The 100-year GWP is used within the Kyoto Protocol of the United Nations Framework Convention on Climate Change to place emissions on a common scale and IPCC (see e.g. Forster *et al.*[8]) regularly reports 20, 100 and 500 year

GWP values for a large number of gases. The GWP is just one possible climate metric to place emissions on a CO_2-equivalent scale (see *e.g.* Fuglestvedt *et al.*[50]) but we present GWPs for consistency with the earlier literature

Using the lifetimes reported in Section 3.2 and RE values given in Section 3.4, Table 5 presents the GWP for these time horizons, using the absolute GWPs for CO_2 given in Forster *et al.*[8]. The values in Table 5 will differ from those available in Forster *et al.*[8] because of differences in the lifetime and RE values reported in previous sub-sections – note in particular the use of a temperature of 272 K to calculate the lifetime, will lead to longer lifetimes than those studies that had used room temperature reaction rates. In some cases, the agreement with earlier literature can result form a fortuitous cancellation of differences between the RE and the lifetime.

Table 5 shows that the 100-year GWP is considerably higher than that of CO_2 for all gases, particularly for the two gases, HFE-7000 and HFE-7100, with longer lifetimes. The values are, though, much smaller than those of the much-longer lived CFCs – for example the 100-year GWP for CFC-11 is 4730. Comparing the 100-year GWP values with those in Forster *et al.*[8], for HFE-7200 our value is 17% larger, because of the longer lifetime in our calculations, our HFE-7100 is 13% higher, because of a longer lifetime, and our HFE-7000 is 13% lower, due a combination of lower RE and lower lifetime. Forster *et al.*[8] do not report a value for $C_3F_7CH_2OH$.

In summary, we have very carefully examined the atmospheric lifetimes and lifetime-corrected REs of these compounds, and therefore believe that the GWPs we derive for these compounds are the best currently available.

4. Conclusion

Rate coefficients as a function of temperature have been determined for the reactions of OH with a range of HFEs and a fluorinated alcohol. The room-temperature data are in good agreement with previous measurements, obtained using different techniques and under different conditions. In addition, quantitative infrared absorption spectra of these compounds have been obtained and combined with the simple model of Pinnock *et al.*[5] to determine radiative efficiencies for the compounds. Combining these results with the kinetic data allows the determination of their GWPs, which are considerably smaller than those for the CFCs that they have been manufactured to replace. The REs and GWPs are for the most part in reasonable agreement with previous calculations; however, we believe that our values represent the best determinations of these quantities at the present time.

5. Acknowledgments

We thank the Spanish Ministry of Science-Education (project CGL2007-62479/CLI) and the Castilla-La Mancha Science-Education Council (project PAI06-0030-3769) for their financial support. We also thank Dr. Andrés Moreno for the determination of the composition of the HFEs. We thank 3M for supplying samples of the HFEs.

6. References

[1] WMO, 2003: *Scientific Assessment of Ozone Depletion: 2002.* Global Ozone Research and Monitoring Project Report No. 47, World Meteorological Organisation, Geneva, 498 pp.

[2] EPA, U.S. Environmental Protection Agency. Clean Air Act. http://www.epa.gov/ozone/snap/index.html

[3] 3M™ Novec™ Engineered Fluids. http://www.3M.com.

[4] M. J. Kurylo, V. L. Orkin, *Chemical Reviews* **2003**, *103*, 5049.

[5] S. Pinnock, M. D. Hurley, K. P. Shine, T. J. Wallington, T. J. Smyth, *Journal Of Geophysical Research-Atmospheres* **1995**, *100*, 23227.

[6] K. Tokuhashi, A. Takahashi, M. Kaise, S. Kondo, A. Sekiya, S. Yamashita, H. Ito, *International Journal of Chemical Kinetics* **1999**, *31*, 846.

[7] P. M. D. Forster, J. B. Burkholder, C. Clerbaux, P. F. Coheur, M. Dutta, L. K. Gohar, M. D. Hurley, G. Myhre, R. W. Portmann, K. P. Shine, T. J. Wallington, D. Wuebbles, *Journal of Quantitative Spectroscopy & Radiative Transfer* **2005**, *93*, 447.

[8] P. M. D. Forster, V. Ramaswamy, P. Artaxo, T. Berntsen, R. Betts, D. W. Fahey, J. Haywood, J. Lean, D. C. Lowe, G. Myhre, J. Nganga, R. Prinn, G. Raga, M. Schulz, R. Van Dorland, in *Fourth Assessment Report of the Intergovernmental Panel on Climate Change* (Ed.: S. Solomon), Cambridge, **2007**.

[9] E. Martinez, A. Aranda, Y. Diaz-De-Mera, D. Rodriguez, M. R. Lopez, J. Albaladejo, *Environmental Science & Technology* **2002**, *36*, 1226.

[10] Y. Diaz-de-Mera, A. Aranda, D. Rodriguez, R. Lopez, B. Cabanas, E. Martinez, *Journal Of Physical Chemistry A* **2002**, *106*, 8627.

[11] A. Aranda, Y. Diaz-De-Mera, I. Bravo, D. Rodriguez, A. Rodriguez, E. Martinez, *Environmental Science & Technology* **2006**, *40*, 5971.
[12] IUPAC, IUPAC Subcommittee for Gas Kinetic Data Evaluation for Atmospheric Chemistry.
[13] D. L. Baulch, J. Duxbury, S. J. Grant, D. C. Montague, *Journal of Physical and Chemical Reference Data* **1981**, *10*, 1.
[14] H. H. Grotheer, F. L. Nesbitt, R. B. Klemm, *Journal Of Physical Chemistry* **1986**, *90*, 2512.
[15] J. T. Herron, *Journal of Physical and Chemical Reference Data* **1988**, *17*, 967.
[16] D. P. Starkey, K. A. Holbrook, G. A. Oldershaw, R. W. Walker, *International Journal of Chemical Kinetics* **1997**, *29*, 231.
[17] K. Takahashi, O. Yamamoto, T. Inomata, M. Kogoma, *International Journal of Chemical Kinetics* **2007**, *39*, 97.
[18] M. D. Hurley, T. J. Wallington, G. A. Buchanan, L. K. Gohar, G. Marston, K. P. Shine, *Journal Of Geophysical Research-Atmospheres* **2005**, *110*.
[19] F. Kaufman, *Journal Of Physical Chemistry* **1984**, *88*, 4909.
[20] R. H. Perry, D. W. Green, J. O. Maloney, (Editors), *Handbook of Air Pollution Analysis*, 7 ed., McGraw-Hill, Madrid.
[21] L. K. Christensen, J. Sehested, O. J. Nielsen, M. Bilde, T. J. Wallington, A. Guschin, L. T. Molina, M. J. Molina, *Journal Of Physical Chemistry A* **1998**, *102*, 4839.
[22] N. Oyaro, C. Nielsen, *Asian Chemical Letters* **2003**, *7*, 119.
[23] T. J. Wallington, W. F. Schneider, J. Sehested, M. Bilde, J. Platz, O. J. Nielsen, L. K. Christensen, M. J. Molina, L. T. Molina, P. W. Wooldridge, *Journal Of Physical Chemistry A* **1997**, *101*, 8264.
[24] F. Cavalli, M. Glasius, J. Hjorth, B. Rindone, N. R. Jensen, *Atmospheric Environment* **1998**, *32*, 3767.
[25] Y. Ninomiya, M. Kawasaki, A. Guschin, L. T. Molina, M. J. Molina, T. J. Wallington, *Environmental Science & Technology* **2000**, *34*, 2973.
[26] M. D. Hurley, T. J. Wallington, M. P. S. Andersen, D. A. Ellis, J. W. Martin, S. A. Mabury, *Journal Of Physical Chemistry A* **2004**, *108*, 1973.
[27] K. Tokuhashi, H. Nagai, A. Takahashi, M. Kaise, S. Kondo, A. Sekiya, M. Takahashi, Y. Gotoh, A. Suga, *Journal Of Physical Chemistry A* **1999**, *103*, 2664.
[28] L. Chen, S. Kutsuna, K. Nohara, K. Takeuchi, T. Ibusuki, *Journal Of Physical Chemistry A* **2001**, *105*, 10854.
[29] K. J. Hsu, W. B. Demore, *Journal Of Physical Chemistry* **1995**, *99*, 11141.
[30] Z. Zhang, R. D. Saini, M. J. Kurylo, R. E. Huie, *Journal Of Physical Chemistry* **1992**, *96*, 9301.
[31] V. L. Orkin, R. E. Huie, M. J. Kurylo, *Journal Of Physical Chemistry* **1996**, *100*, 8907.
[32] Y. Diaz-de-Mera, A. Aranda, I. Bravo, D. Rodriguez, A. Rodriguez, E. Moreno, *Environmental Science and Pollution Research* **2008**, *15*, 584.
[33] T. J. Wallington, P. Dagaut, M. J. Kurylo, *Journal Of Physical Chemistry* **1988**, *92*, 5024.
[34] G. Kovacs, T. Szasz-Vadasz, V. C. Papadimitriou, S. Dobe, T. Berces, F. Marta, *Reaction Kinetics and Catalysis Letters* **2005**, *87*, 129.
[35] L. Chen, K. Fukuda, N. Takenaka, H. Bandow, Y. Maeda, *International Journal of Chemical Kinetics* **2000**, *32*, 73.

[36] N. Oyaro, S. R. Sellevag, C. J. Nielsen, *Journal Of Physical Chemistry A* **2005**, *109*, 337.
[37] T. Kelly, V. Bossoutrot, I. Magneron, K. Wirtz, J. Treacy, A. Mellouki, H. Sidebottom, G. Le Bras, *Journal Of Physical Chemistry A* **2005**, *109*, 347.
[38] S. Urata, A. Takada, T. Uchimaru, A. K. Chandra, *Chemical Physics Letters* **2003**, *368*, 215.
[39] S. R. Sellevag, C. J. Nielsen, O. A. Sovde, G. Myhre, J. K. Sundet, F. Stordal, I. S. A. Isaksen, *Atmospheric Environment* **2004**, *38*, 6725.
[40] I. W. M. Smith, *Chemical Reviews* **2003**, *103*, 4549.
[41] R. Atkinson, J. Arey, *Chemical Reviews* **2003**, *103*, 4605.
[42] D. D. Nelson, M. S. Zahniser, C. E. Kolb, H. Magid, *Journal Of Physical Chemistry* **1995**, *99*, 16301.
[43] R. G. Prinn, J. Huang, R. F. Weiss, D. M. Cunnold, P. J. Fraser, P. G. Simmonds, A. McCulloch, C. Harth, P. Salameh, S. O'Doherty, R. H. J. Wang, L. Porter, B. R. Miller, *Science* **2001**, *292*, 1882.
[44] K. Smith, D. Newnham, M. Page, J. Ballard, G. Duxbury, *Journal of Quantitative Spectroscopy & Radiative Transfer* **1996**, *56*, 73.
[45] K. Sihra, M. D. Hurley, K. P. Shine, T. J. Wallington, *Journal Of Geophysical Research-Atmospheres* **2001**, *106*, 20493.
[46] R. Imasu, A. Suga, T. Matsuno, *Journal of the Meteorological Society of Japan* **1995**, *73*, 1123.
[47] C. J. Young, M. D. Hurley, T. J. Wallington, S. A. Mabury, *Journal Of Geophysical Research-Atmospheres* **2008**, *113*.
[48] S. R. Sellevag, B. D'Anna, C. J. Nielsen, *Asian Chemical Letters* **2007**, *11*, 33.
[49] WMO, 1998: *Scientific Assessment of Ozone Depletion: 1998.* Global Ozone Research and Monitoring Project Report No. 44, World Meteorological Organisation, Geneva.
[50] J. S. Fuglestvedt, K. P. Shine, J. Cook, T. Bernsten, D. S. Lee, A. Stenke, R. B. Skeie, G. J. M. Velders, I. A. Waaitz, *Atmospheric Environment* **2009**.

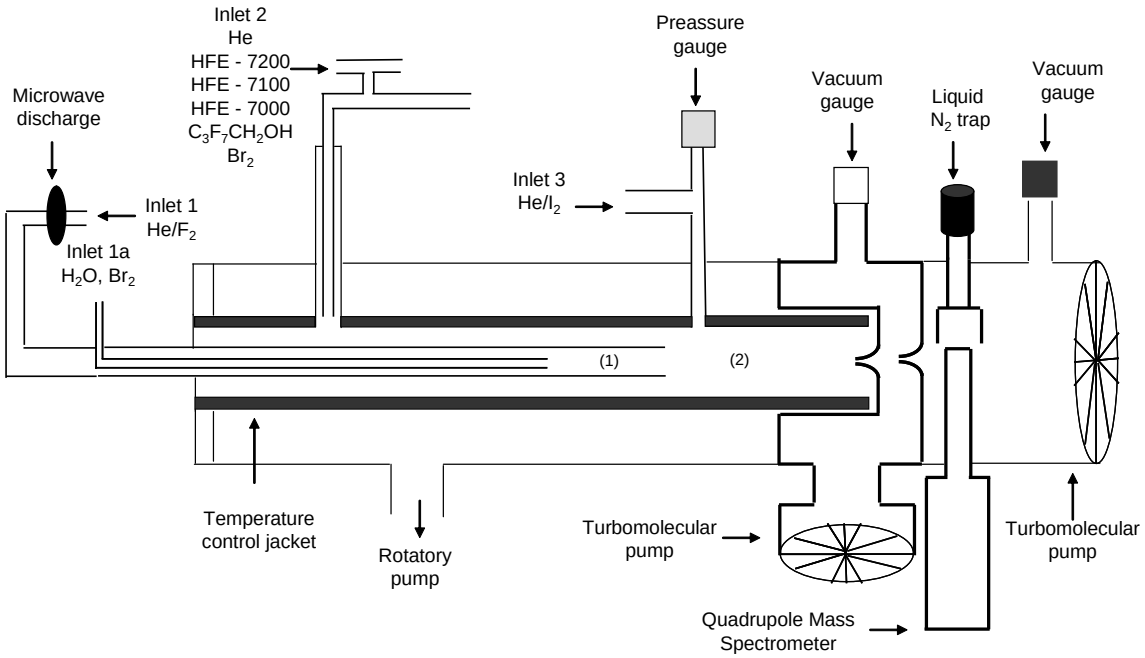

Figure 1. Schematic view of the experimental set-up

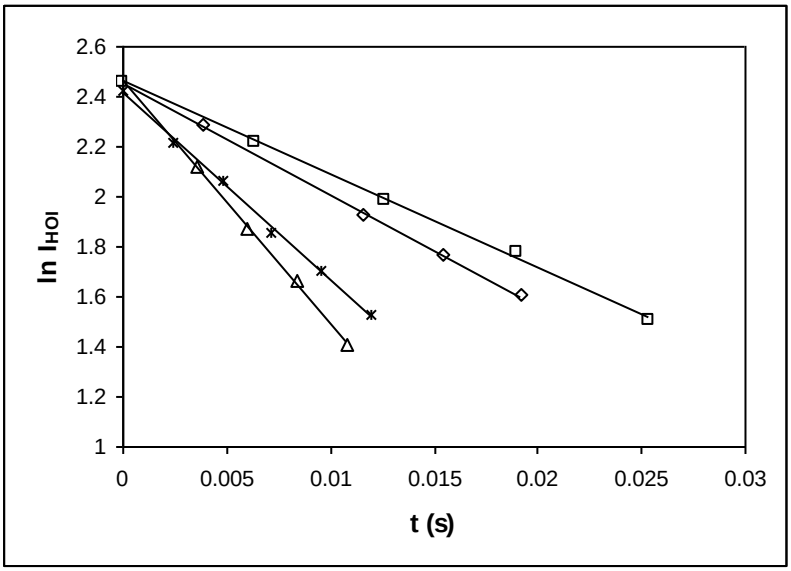

Figure 2. Typical pseudo-first-order decays of HOI for the OH + $C_3F_7CH_2OH$ reaction at 298 K and 1 Torr: [$C_3F_7CH_2OH$]=1.60 (□); 2.16 (◊); 5.59 (∗); 7.44 (Δ) x 10^{14} molecule cm^{-3}.

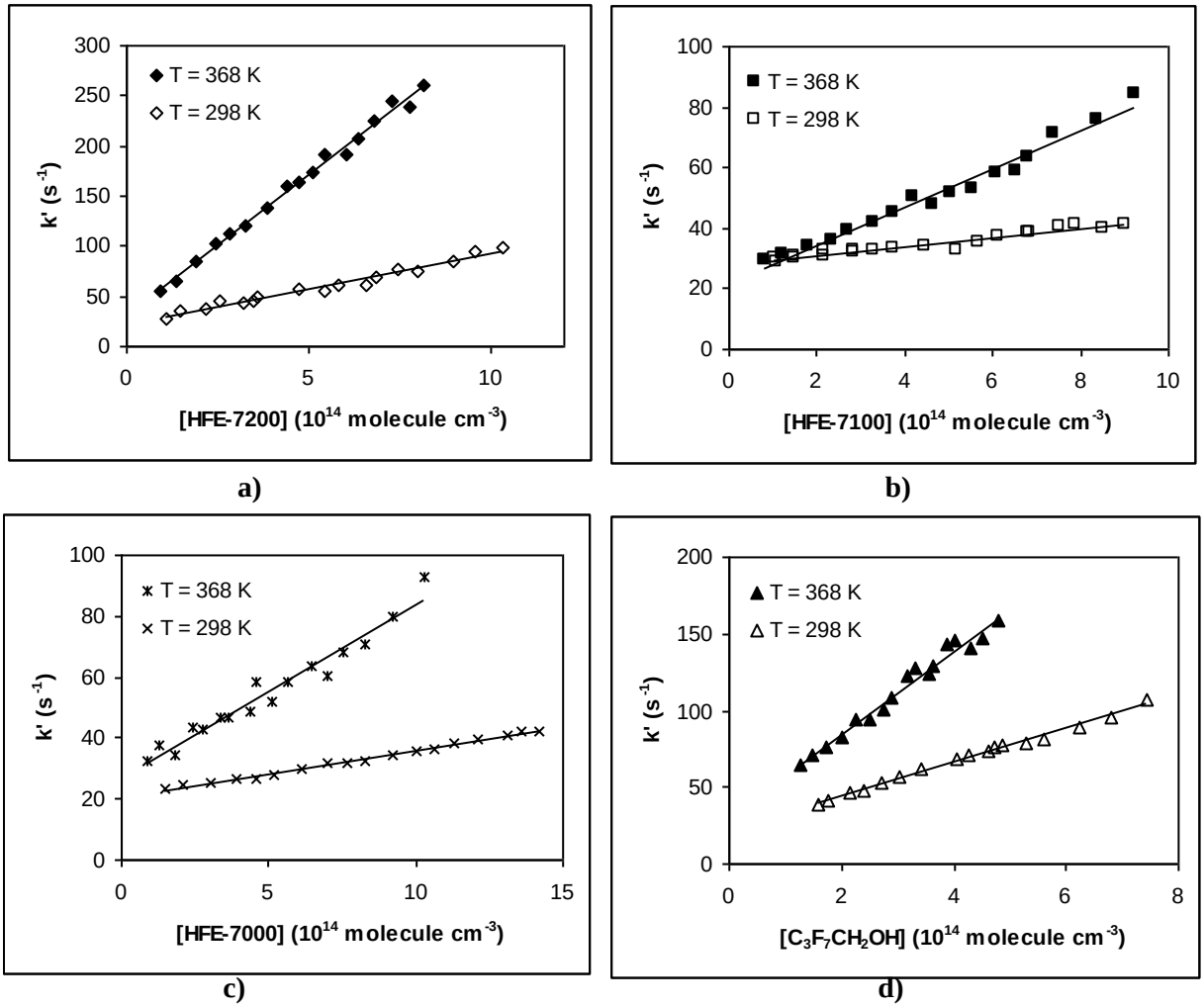

Figure 3. Plots of the pseudo first order rate constants, k', versus the CFCs substitute concentration at p=1 Torr and different temperatures: a) HFE-7200, b) HFE-7100, c) HFE-7000, and d) $C_3F_7CH_2OH$.

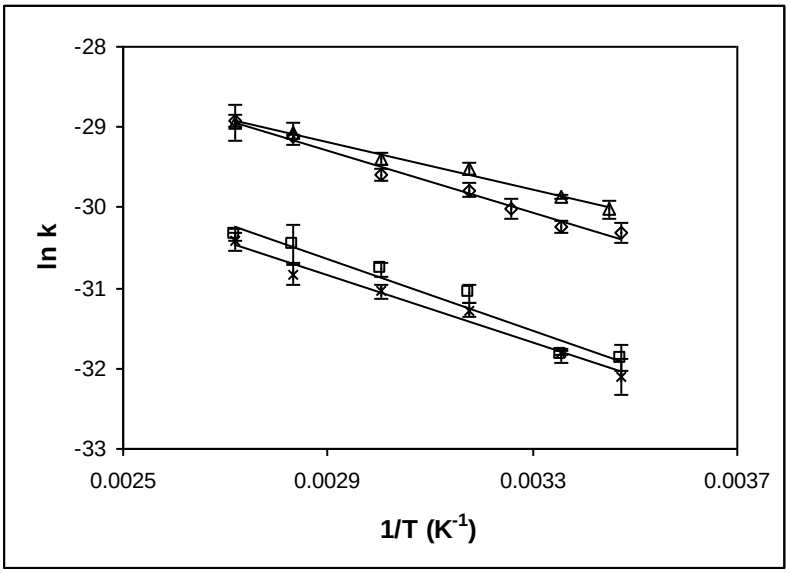

Figure 4. Temperature dependence of the reaction rate constants: OH + HFE-7200 (◊), OH + HFE-7100 (□), OH + HFE-7000 (×), and OH + $C_3F_7CH_2OH$ (Δ). Errors are 2σ.

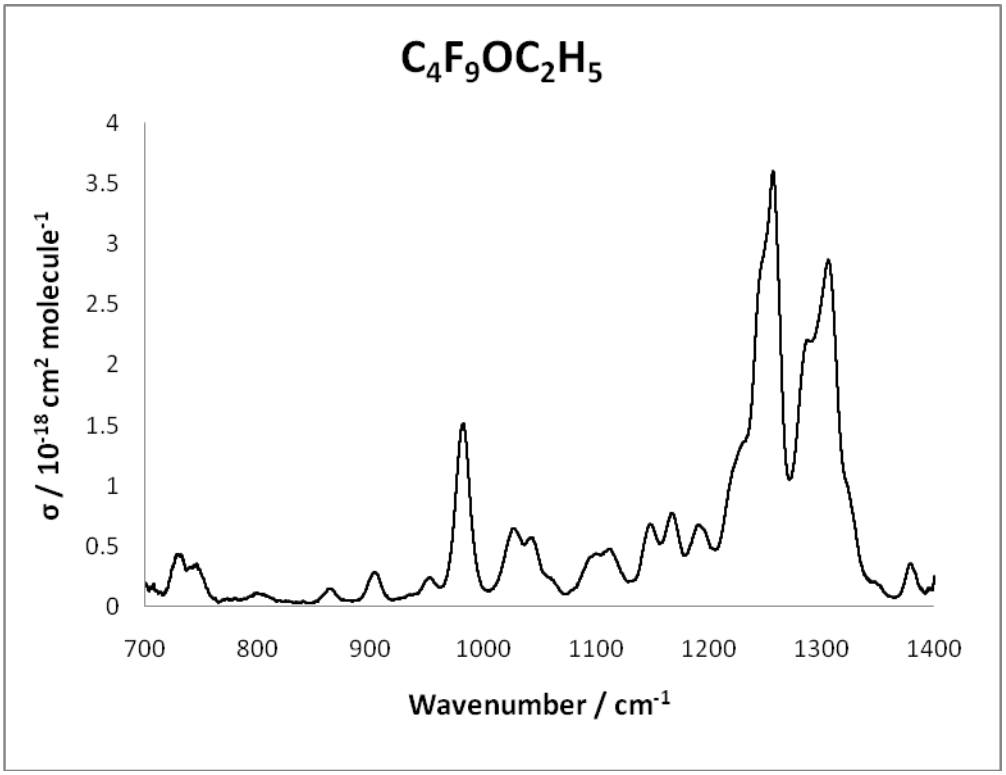
C4F9OC2H5
σ / 10-18 cm2 molecule-1
4
3.5
3
2.5
2
1.5
1
0.5
0
700
800
900
1000
1100
1200
1300
1400
Wavenumber / cm-1

Figure 5a

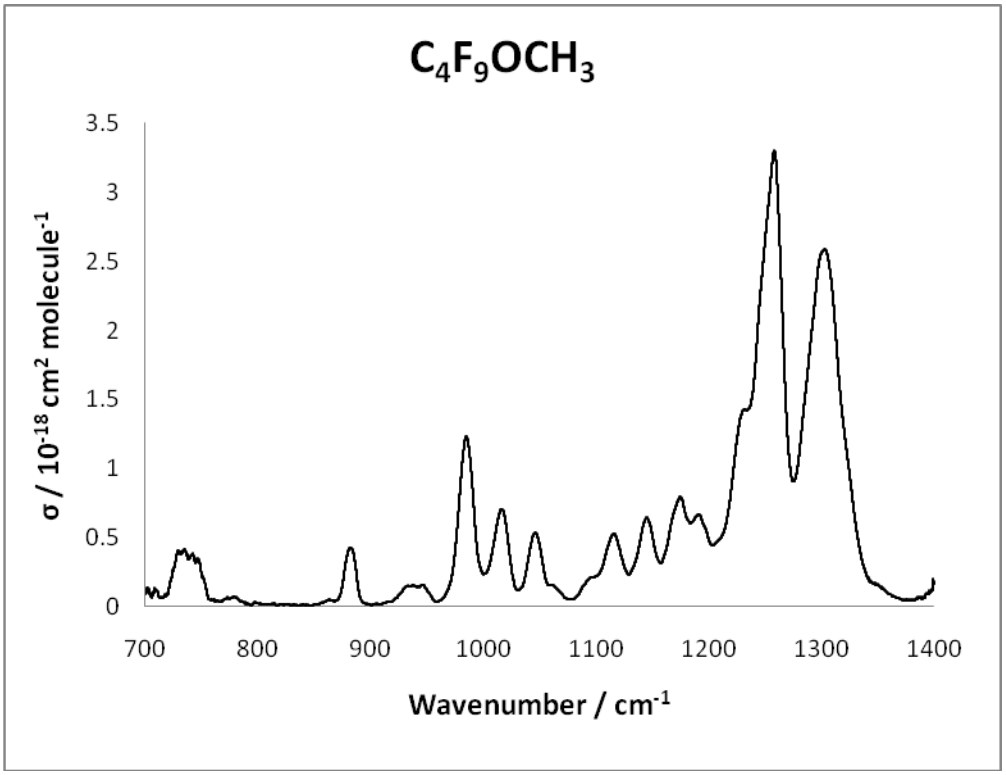
C4F9OCH3
σ / 10-18 cm2 molecule-1
3.5
3
2.5
2
1.5
1
0.5
0
700
800
900
1000
1100
1200
1300
1400
Wavenumber / cm-1

Figure 5b

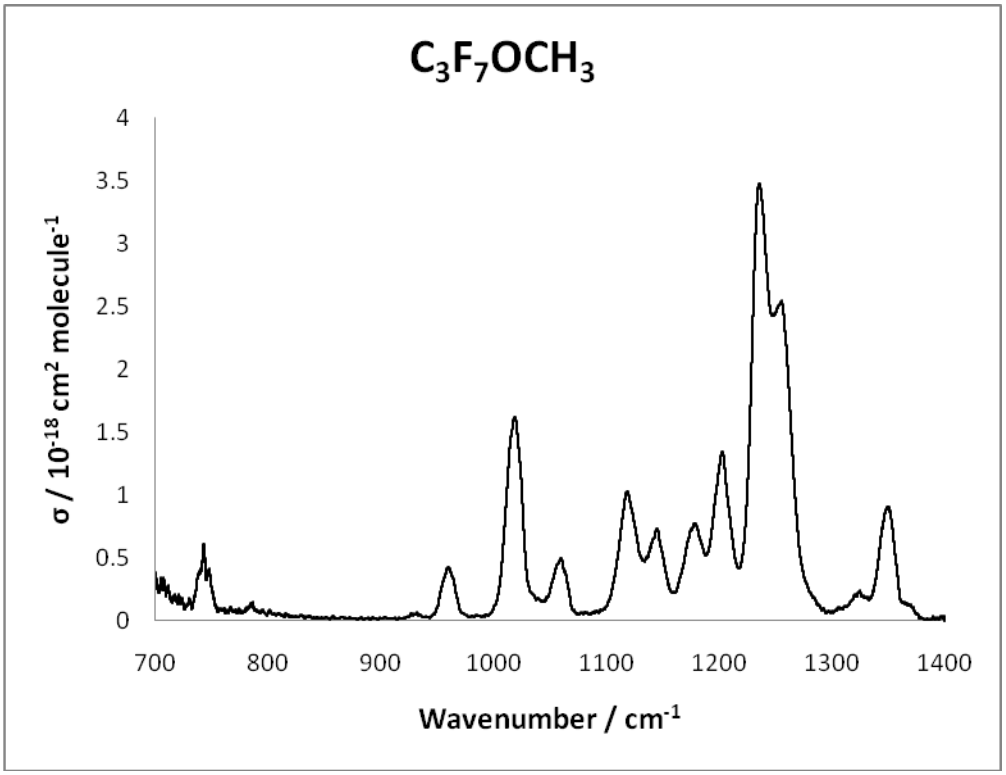
C3F7OCH3
σ / 10-18 cm2 molecule-1
4
3.5
3
2.5
2
1.5
1
0.5
0
700
800
900
1000
1100
1200
1300
1400
Wavenumber / cm-1

Figure 5c

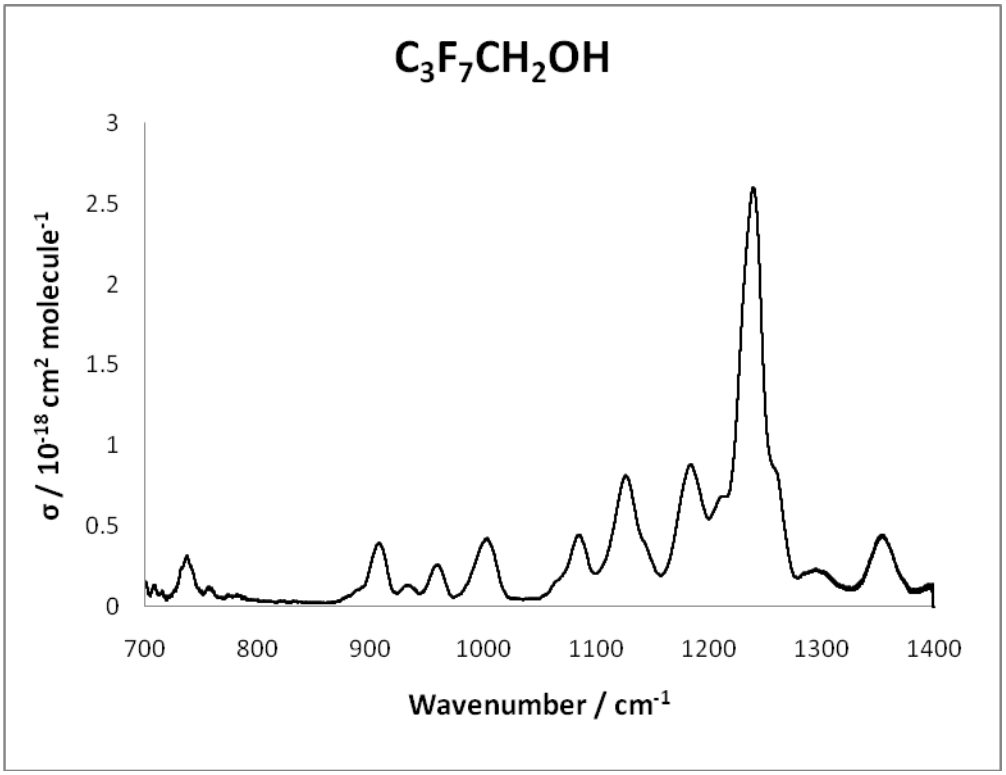

Figure 5d

Figure 5. Infrared spectra of: (a) HFE-7200; (b) HFE-7100; (c) HFE-7000; and (d) $C_3F_7CH_2OH$. Spectra have been smoothed to *ca* 2 cm^{-1} resolution using a sliding average method.

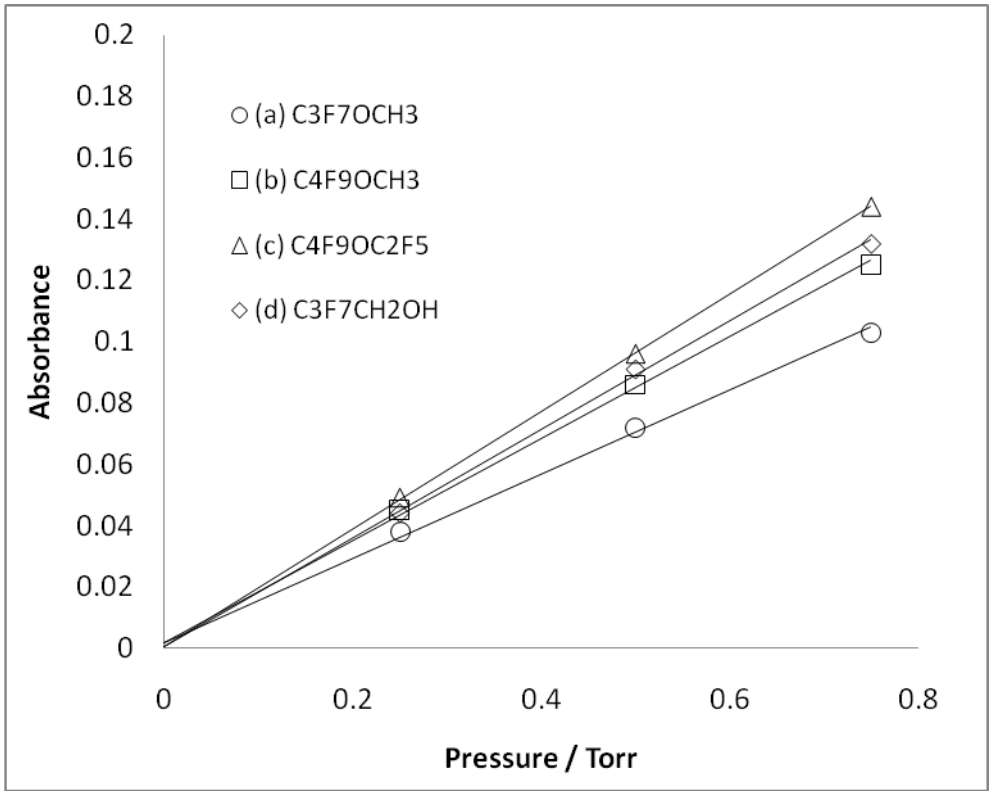

Figure 6. Plots of absorbance *vs*. pressure for: (a) HFE-7000 (at 1237 cm^{-1}); (b) HFE-7100 (at 1304 cm^{-1}); (c) HFE-7200 (at 1309 cm^{-1}); and (d) $C_3F_7CH_2OH$ (at 1243 cm^{-1}).

Table 1. Experimental conditions for the determination of the rate coefficients at different temperatures measured in region (2) of the experimental set-up.

Experimental Conditions	*HFE-7200*	*HFE-7100*	*HFE-7000*	$C_3F_7CH_2OH$
T (K)	288-368			
p (Torr)	1			
Flow velocity (m s^{-1})	780-1016	760-1030	780-1320	760-1000
Reaction time (ms)	6-30	10-35	10-32	6-20
[F_2] (10^{12} molecule cm^{-3})	2-12	3-9	2.2-9	4-10
[H_2O] (10^{14} molecule cm^{-3})	0.5-1.0	0.5-1.6	0.5-1.3	0.5-1.3
[CFC substitute] (10^{14} molecule cm^{-3})	0.9-12	0.8-11.3	0.9-22	1.2-7.4

Table 2. Summary of the second-order rate constants obtained in this work for the reactions of OH radicals with the CFCs substitutes studied. Units of cm^3 $molecule^{-1}$ s^{-1}, errors are at 2σ.

T / K	***HFE-7200***	***HFE-7100***	***HFE-7000***	***$C_3F_7CH_2OH$***
288	$(6.88\pm0.83)\times10^{-14}$	$(1.44\pm0.23)\times10^{-14}$	$(1.15\pm0.26)\times10^{-14}$	
290				$(9.12\pm1.71)\times10^{-14}$
298	$(7.32\pm0.55)\times10^{-14}$	$(1.49\pm0.13)\times10^{-14}$	$(1.54\pm0.05)\times10^{-14}$	$(1.07\pm0.05)\times10^{-13}$
307	$(9.26\pm1.22)\times10^{-14}$			
315	$(1.16\pm0.10)\times10^{-13}$	$(3.24\pm0.36)\times10^{-14}$	$(2.62\pm0.21)\times10^{-14}$	$(1.51\pm0.18)\times10^{-13}$
333	$(1.41\pm0.12)\times10^{-13}$	$(4.33\pm0.41)\times10^{-14}$	$(3.29\pm0.25)\times10^{-14}$	$(1.72\pm0.14)\times10^{-13}$
353	$(2.26\pm0.07)\times10^{-13}$	$(5.90\pm1.51)\times10^{-14}$	$(4.09\pm0.54)\times10^{-14}$	$(2.35\pm0.18)\times10^{-13}$
368	$(2.73\pm0.20)\times10^{-13}$	$(6.64\pm0.48)\times10^{-14}$	$(6.15\pm0.70)\times10^{-14}$	$(2.67\pm0.28)\times10^{-13}$

Table 3. Rate constants for the reaction between the OH radical and the title compounds at 298K. All the results are given with 2σ uncertainties.

Compound	*Isomer*	*k (cm^3 $molecule^{-1}$ s^{-1})*	*Conditions*	*Reference*
$C_4F_9OC_2H_5$ (HFE-7200)	n-$C_4H_9OC_2H_5$	$(6.4\pm0.7)\times10^{-14}$	RR, 200 Torr He	[21]
	i- $C_4H_9OC_2H_5$	$(7.7\pm0.8)\times10^{-14}$	RR, 200 Torr He	[21]
	Mixture	$(1.00\pm0.03)\times10^{-13}$	RR, 1 atm air	[22]
	Mixture	$(7.32\pm0.55)\times10^{-14}$	DF, 1 Torr He	This work
$C_4F_9OCH_3$ (HFE-7100)	Mixture	$\sim1.2\times10^{-14}$	RR, 200 Torr He	[23]
	Mixture	$(7.2\pm1.6)\times10^{-15}$	RR, 740 Torr, Air	[24]
	Mixture	$(1.48\pm0.07)\times10^{-14}$	RR, 1 atm air	[22]
	Mixture	$(1.49\pm0.13)\times10^{-14}$	DF, 1 Torr He	This work
***n*-$C_3F_7OCH_3$ (HFE-7000)**	n-$C_3H_7OCH_3$	$(1.18\pm0.05)\times10^{-14}$	FP / LP, 20-60 Torr He DF, 4-6 Torr He	[6]
	i-$C_3H_7OCH_3$	$(1.52\pm0.06)\times10^{-14}$	FP / LP, 20-60 Torr He DF, 4-6 Torr He	[6]
	n-$C_3H_7OCH_3$	$(1.2\pm0.3)\times10^{-14}$	RR, 200 Torr He	[25]
	n-$C_3H_7OCH_3$	$(1.54\pm0.05)\times10^{-14}$	DF, 1 Torr He	This work
$C_3F_7CH_2OH$	N/A	$(1.02\pm0.10)\times10^{-13}$	RR, 700 Torr air	[26]
	N/A	$(1.07\pm0.05)\times10^{-13}$	DF, 1 Torr He	This work

RR: Relative Rate. DF: Discharge Flow. FP / LP: Flash Photolysis / Laser Photolysis

Table 4. Atmospheric lifetimes of HFE-7200, HFE-7100, HFE-7000 and $C_3F_7CH_2OH$

Compound	k_{OH} *(298K)*[a]	τ_{OH}*(298K)*[b] */ year*	k_{OH} *(272K)*[c]	τ_{OH} *(272K)*[d] */ year*
HFE-7200	$(7.32\pm0.27)\times10^{-14}$	0.43±0.02	$(3.96\pm1.79)\times10^{-14}$	0.91±0.41
HFE-7100	$(1.49\pm0.06)\times10^{-14}$	2.1±0.1	$(8.60\pm10.2)\times10^{-15}$	4.2±4.9
HFE-7000	$(1.54\pm0.02)\times10^{-14}$	2.1±0.1	$(7.95\pm5.6)\times10^{-15}$	4.5±3.2
$C_3F_7CH_2OH$	$(1.07\pm0.02)\times10^{-13}$	0.30±0.01	$(6.53\pm1.88)\times10^{-14}$	0.55±0.16

[a]This work. [b]From $\tau=1/k[OH]$ [c]Derived from the Arrhenius expressions obtained in this work. [d]From equation II. *k* in units of cm^3 $molecule^{-1}$ s^{-1}. Errors are σ.

Table 5. Integrated Absorption Cross Sections (600-1800 cm^{-1}), Radiative Forcing Efficiencies (RE) — for a constant mixing ratio profile and lifetime-corrected — and GWPs, relative to CO_2, for HFE-7200, HFE-7100, HFE-7000 and $C_3F_7CH_2OH$.

Compound	$S(T)$[a]	RE[b]	Lifetime corrected RE[b]	Lifetime[c]	GWPs		
					20 yr	100 yr	500 yr
HFE-7200	38.6 ± 5.8	0.42	0.31	0.91	243	69	21
HFE-7100	34.5 ± 8.3	0.36	0.31	4.2	1180	337	102
HFE-7000	28.1 ± 7.2	0.37	0.32	4.8[d]	1730	499	152
$C_3F_7CH_2OH$	21.5 ± 4.0	0.28	0.20	0.55	126	36	11

[a] Units are 10^{-17} cm^2 $molecule^{-1}$ cm^{-1}; [b] Units are W m^{-2} $ppbv^{-1}$. [c] Units are yr. [d] Derived from an average of our k_3(272 K) value and that of Tokuhashi *et al.*[6]